Separating climate-induced mass transfers and instrumental effects from tectonic signal in repeated absolute gravity measurements

Michel van Camp, Olivier de Viron, Jean-Philippe Avouac

Separating climate-induced mass transfers and instrumental effects from tectonic signal in repeated absolute gravity...

Article *in* Geophysical Research Letters · May 2016

DOI: 10.1002/2016GL068648

CITATION
1

READS
92

3 authors:

Michel Van Camp
Royal Observatory of Belgium
110 PUBLICATIONS **957** CITATIONS
SEE PROFILE

Olivier De Viron
Université de La Rochelle
191 PUBLICATIONS **1,203** CITATIONS
SEE PROFILE

Jean-Philippe Avouac
California Institute of Technology
373 PUBLICATIONS **13,465** CITATIONS
SEE PROFILE

Separating climate-induced mass transfers and instrumental effects from tectonic signal in repeated absolute gravity measurements

M. Van Camp[1], O. de Viron[2], J. P. Avouac[3]

[1]Royal Observatory of Belgium
Sismology-Gravimetry
Avenue Circulaire, 3
BE-1180 Uccle

[2]Littoral, Environnement et Sociétés (LIENSs), Université de La Rochelle and CNRS (UMR7266)

[3] Geological and Planetary Science Division, Caltech Institute of Technology, Pasadena, USA

Corresponding author: Michel Van Camp (mvc@oma.be)

Key Points:

- The signature of climate-induced interannual mass transfers on repeated absolute gravity measurements is estimated everywhere in the world
- Instrumental artefacts should be taken into account and mitigated as much as possible.
- In most cases, the uncertainty is estimated to ~5 nm/s²/a after 10 yearly campaigns

Abstract 150 words

We estimate the signature of the climate-induced mass transfers in repeated absolute gravity measurements based on satellite gravimetric measurements from the GRACE mission. We show results at the globe scale, and compare them with repeated absolute gravity (AG) time behavior in three zones where AG surveys have been published: Northwestern Europe, Canada and Tibet. For 10 yearly campaigns, the uncertainties affecting the determination of a linear gravity rate of change range 3-4 nm/s²/a in most cases, in absence of instrumental artefacts. The results are consistent with what is observed for long term repeated campaigns. We also discuss the possible artifact that can results from using short AG survey to determine the tectonic effects in a zone of high hydrological variability. We call into question the tectonic interpretation of several gravity changes reported from stations in Tibet, in particular the variation observed prior to the 2015 Gorkha earthquake.

1 Introduction

Absolute gravimeters (AG), by construction, suffer no time drift; this makes them most appropriate to measure long-term surface gravity changes, which might reflect either vertical ground motion or mass redistribution. AGs have for example been used to monitor slow vertical ground displacements [*Mazzotti* et al., 2007; *Djamour* et al., 2010; *Van Camp* et al., 2011; *Zerbini* et al., 2007] and Glacial Isostatic Adjustment [*Lambert* et al., 2006; *Steffen* et al., 2009; *Mazzotti* et al., 2011; *Sato* et al., 2012]. It has also been used to study mass redistribution by erosion [*Mouyen* et al., 2013] and crustal tectonics [*Mouyen* et al., 2014]. Intriguing measurements of gravity changes in Tibet have been recently reported: Sun et al [2009] found evidences for a gravity decrease at three stations, which they interpreted as the signature from a long term thickening of the Tibetan plateau and *Chen et al.* [2015] reported a gravity increase,

which they attribute to preseismic processes associated to the 2015, Mw 7.8 Gorkha earthquake. Such tectonic interpretation should be considered with caution in view of the possible effect of non-tectonic causes, in particular surface hydrology, on absolute gravity measurements and instrumental artefacts. *Yi et al.* [2016] showed that the signal observed prior to the Gorkha earthquake by *Chen et al.* [2015] is most probably due to a local hydrological effect unrelated to the earthquake itself.

Gravity measurements are indeed extremely sensible to local water storage changes, which depends on very local geologic and climatic conditions, e.g. rock porosity, vegetation, evaporation, and runoff rates [*Van Camp* et al., 2006a; *Jacob* et al., 2008; *Creutzfeldt* et al., 2010a; *Lampitelli and Francis*, 2010]; the associated gravimetric signature often exceeds the tectonic effects, and consequently induces non negligible time correlated signature in the gravity time series [*Van Camp* et al., 2010]. Hydrological effects are observed locally from AG measurements but also at the regional or global scale from satellite gravimetric measurements or GPS geodetic measurements [e.g. *Bettinelli et al.*, 2008, *Blewitt et al.*, 2001; *Chanard et al.*, 2014; *Ramillien et al.*, 2004; *van Dam et al.*, 2001].

Separating the instrumental artifacts and the contribution of surface hydrology from tectonic processes in the AG measurements is thus a major challenge. A better understanding and quantification of these effects, as well as of instrumental artifacts, is in our view a prerequisite to any tectonic interpretation of an AG survey. Hereafter, we first discuss instrumental artifacts and next discuss hydrological effects based on satellite gravimetric measurements and comparison with local AG observations in a few areas.

2 Instrumental artefacts

When different AGs are used in the same study, inter-instrument differences should be taken into account, as done for example by *Lambert* et al. [2006; 2013b], or included in the uncertainty budget [*Sato et al.* 2006; *Mémin et al.*, 2011, *Palinkas et al.*, 2012]. Intercomparison campaigns [e.g. *Francis* et al., 2005; 2010; 2013; 2015; *Jiang* et al., 2012; *Schmerge* et al., 2012; *Vitushkin* et al., 2002] showed that differences between FG5 and JILAg gravimeters are commonly of the order of 100-150 nm/s² . A difference as large as 461 nm/s² was reported for one of the A10 instruments that participated in the ICAG-2001 intercomparison [*Vitushkin* et al., 2002]. In other comparisons, systematic and random errors of A10 gravimeters ranged between 70 and 220 nm/s² [*Jiang* et al., 2011; *Francis* et al., 2005; 2013; 2015].

Concurrently, the uncertainty due to the setup of the AG instrument should be taken into account. This noise results from instrumental setup-dependent offsets and can be due for example to middling alignment of the instrument, errors in height measurement, slight perturbations due to transportation or different instrument-floor couplings. For an FG5, the sources of uncertainties can be represented by a normal random distribution, with a standard deviation of 16 nm/s² [*Van Camp* et al., 2005]. In some circumstances, larger, isolated systematic errors due to instrumental setup may occur. For example, an error in the laser frequency can induce a shift in gravity of 270 nm/s²; a malfunctioning or not calibrated clock is also possible (2 nm/s²/mHz for an FG5 instrument), etc. (for a comprehensive review of errors see *Niebauer* et al. [1995]). This is difficult to detect but can be mitigated by sufficiently repeating the AG measurements. Finally, other possible artefacts like building construction or soil sealing around the gravity station may modify gravity significantly.

3 Separating hydrological effects from tectonic signal

Separating hydrological signature from tectonic signal in AG data can be done if either (1) the hydrological signal is known with a precision sufficient to allow subtraction of the hydrology signature from the AG data, (2) one disposes from sensors with a response to hydrological load and tectonic effect different from that of the AG, or (3) the space-time behavior of the two signals differs to such an extent that it is possible to use data processing technique to separate them. The third method is most often not practical because of the sparsity in time and space of AG data. Method 2 requires disposing of additional data of a different kind.

Method 1 requires precise independent information about hydrology. Estimating subsurface water storage changes is notoriously complex, and it is even more so at the very local scale, where the gravity transfer function is the most sensible. *Lambert* et al. [2006] succeeded in that estimation using a single-thank soil moisture model, but this method is not easily transposable. Such a modeling of hydrogeological effects requires comprehensive investigations and costly in situ instrumentation for ground water measurements [*Creutzfeldt* et al., 2010a; 2010b], which cannot be performed at each gravity station. In addition, correction of the hydrology signature by applying global hydrological models such as the Global Land Data Assimilation System [GLDAS, *Rodell* et al., 2004] or European Re-Analysis [ERA, *Uppala* et al., 2005], or space-based observations from the Gravity Recovery and Climate Experiment [GRACE, *Wouters* et al., 2014] is not adequate, given their limited time and space resolution. Ground water storage is indeed heterogeneous in space and variable in time at scales below the spatial and temporal resolution of GRACE, preventing one from retrieving local hydrological effects [*Van Camp* et al., 2010; 2014].

Separation of the causes of temporal variations of AG measurements and precise correction of hydrogeological effects is thus not possible in most cases. Based on the spectral content of modelled hydrogeological effects and of SG time series, *Van Camp* et al. [2011] investigated the hydrological effects on repeated gravity measurements. They showed that the time required to measure a gravity rate of change of 1 nm/s²/a at the 1σ level was of the order of 10 years but highly dependent on the location, assuming continuous, hourly sampled gravity time series at the existing SG stations. In case of repeated absolute gravity measurements, the continuity of measurements is broken, and the setup noise must be taken into account. Presently, the easiest and only practical way to mitigate hydrological effects in AG measurements is to perform measurements at the same epoch of the year –the impact of seasonal variations is then minimized and, for a sufficiently long time period, interannual variations average out. This procedure is only approximate due to long-term variability of the hydrological signal and to possible long term drift of groundwater storage. The addition of superconducting gravimeter (SG) information mitigates the error in the estimation of gravity rates of change caused by the presence of long period, interannual, and annual signals in the AG data [*Van Camp et al.*, 2013], but this remains unpractical. However, global models, as GRACE or GLDAS, can meaningfully be used to investigate the spatiotemporal behavior of the hydrological signal, and gather information about the possible magnitude of the hydrological signature.

Since 2002, GRACE has provided long enough time series to be used as in the study of *Van Camp et al.* [2010]. Unlike most of the global hydrological model, GRACE integrates the whole ground water content, from the saturated and unsaturated zones, producing a reliable tool to estimate water storage changes. Hence, keeping in mind that the local effects can significantly modify the water storage change signal both in phase and amplitude [*Van Camp et al.*, 2014],

GRACE can be used as a proxy in order to estimate the space-time variability of water storage changes in different climatic and hydrogeological contexts on repeated gravity measurements. This is done below by simulating repeated AG measurements performed once a year.

4 Space-time variability of hydrological effects on surface gravity measurements

We use monthly GRACE mass concentration (mascon) solutions from JPL [*Watkins* et al., 2015; *Wiese* et al., 2015]. The solutions are expressed on a 0.5 by 0.5 degree grid, though the actual resolution is closer to 2 degrees. As we want to avoid the influence of possible slow tectonic processes, a 1st-degree polynomial estimated at each point over the whole GRACE area, was removed, to avoid the influence of possible slow tectonic processes.

In this study, we only consider the Newtonian effects on the AG measurements. The deformation effect caused by the surface mass loading can be corrected using Global Navigation Satellite System (GNSS) observations [*Zerbini et al.*, 2007] and, after 5 years, is at the mm/a level [*Santamaría-Gómez and Mémin,* 2015], equivalent to 3 nm/s²/a.

The equivalent water height is converted into gravity signal, in nm/s², using the Bouguer factor of 4.2 nm/s² for 1 cm of water height equivalent, which has been shown to be an excellent approximation [*Creutzfeldt* et al., 2008]. Then, we computed the Allan standard deviation [*Allan*, 1966], i.e. the averaged squared differences between successive averages performed over a given time interval as a function of the interval length.

$$\sigma_y^2(\tau) = \frac{1}{2}\langle\left(\bar{y}_{n+1,\tau} - \bar{y}_{n,\tau}\right)^2\rangle,$$

where the averages $\bar{y}_{n+1,\tau}$ are computed over the interval τ.

This statistics quantifies the impact of the timescale τ on the variability of the signal. This was done on each grid cell everywhere on land but Antarctica and Greenland, for which there is no solution of the JPL mascon.

The Allan deviations of the gravity signature are calculated for time intervals of 12 months over three zones where several studies reporting on repeated AG measurements were published (Figure 1): Northwestern Europe (Belgium and western Germany; *Van Camp* et al. [2011], results extended to 2014 by the authors), Canada-Northern USA [*Lambert* et al., 2006; 2013a; 2013b; *Mazzotti* et al., 2011] and Southeast Asia (Tibet; *Sun* et al. [2009]; *Chen* et al. [2016]). This is also done at time intervals of 1, 3, 6 and 60 months for the whole world (Figure 2). Note that the color scale has been saturated to allow a better visibility. In the supporting information, Figures S1 show other zones not discussed in this paper: Central Asia, South America, Africa and Oceania. Figure S2 provides the distributions shown on Figures 1 and S1.

The figures indicate that, in most of the cases, we can expect a standard deviation in the range 10-25 nm/s² for measurements repeated once a year, due to interannual climate dynamics. In other words, even when performing the measurements at the same moment every year, the 95% confidence interval for the interannual gravity variability, for example due to hydrological-related surface load variations, is typically in the interval 20-50 nm/s².

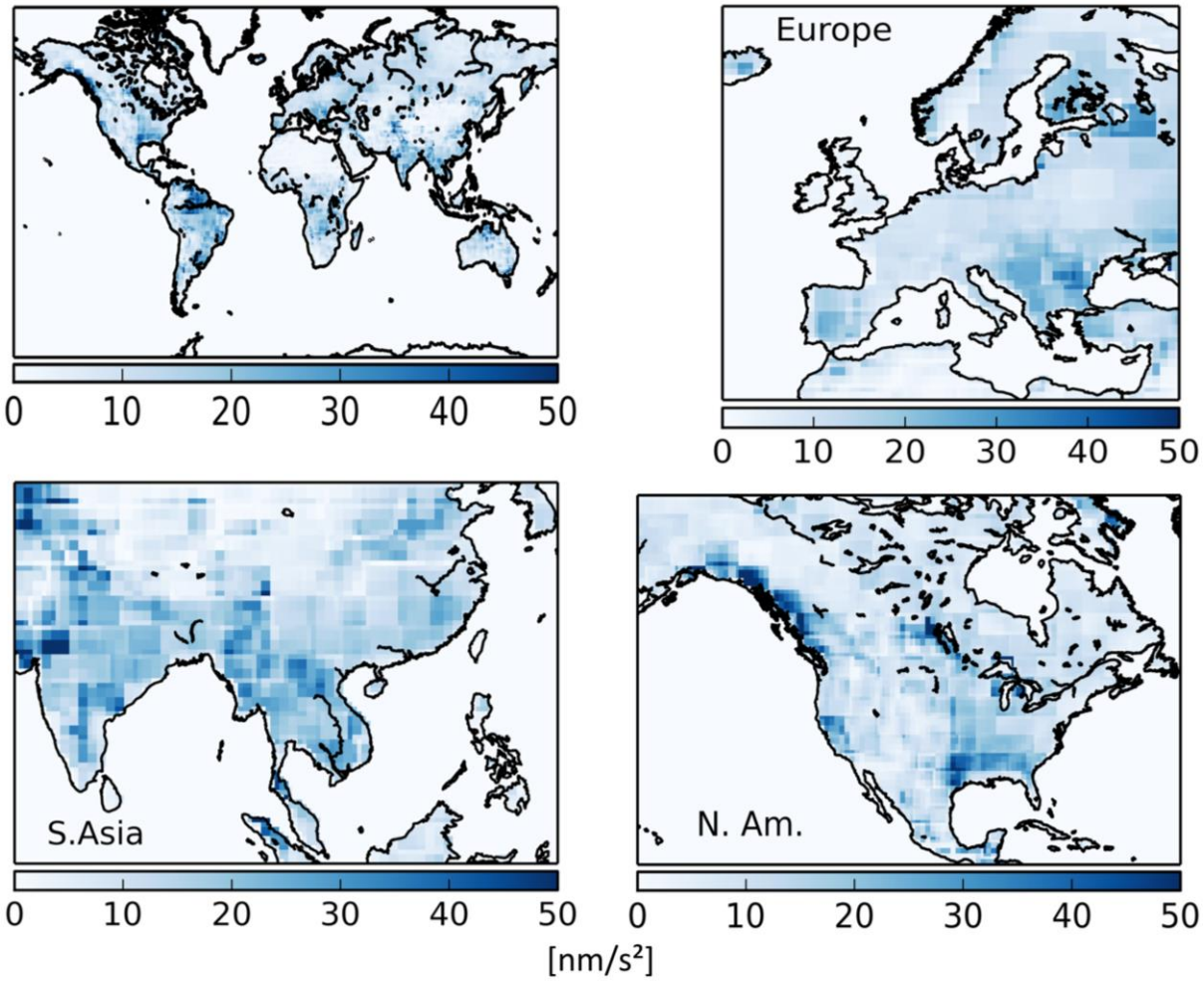

Figure 1. Allan deviations of the hydrological effects on repeated gravity measurements, at the period of 12 months, which indicate the interannual variability in the whole world, Europe, Southeast Asia and North America. The hydrological effects are computed using GRACE observations, using the Bouguer conversion ratio of 4.2 nm/s² per cm of water. See Figures S1 for South America, Central Asia, Africa and Oceania.

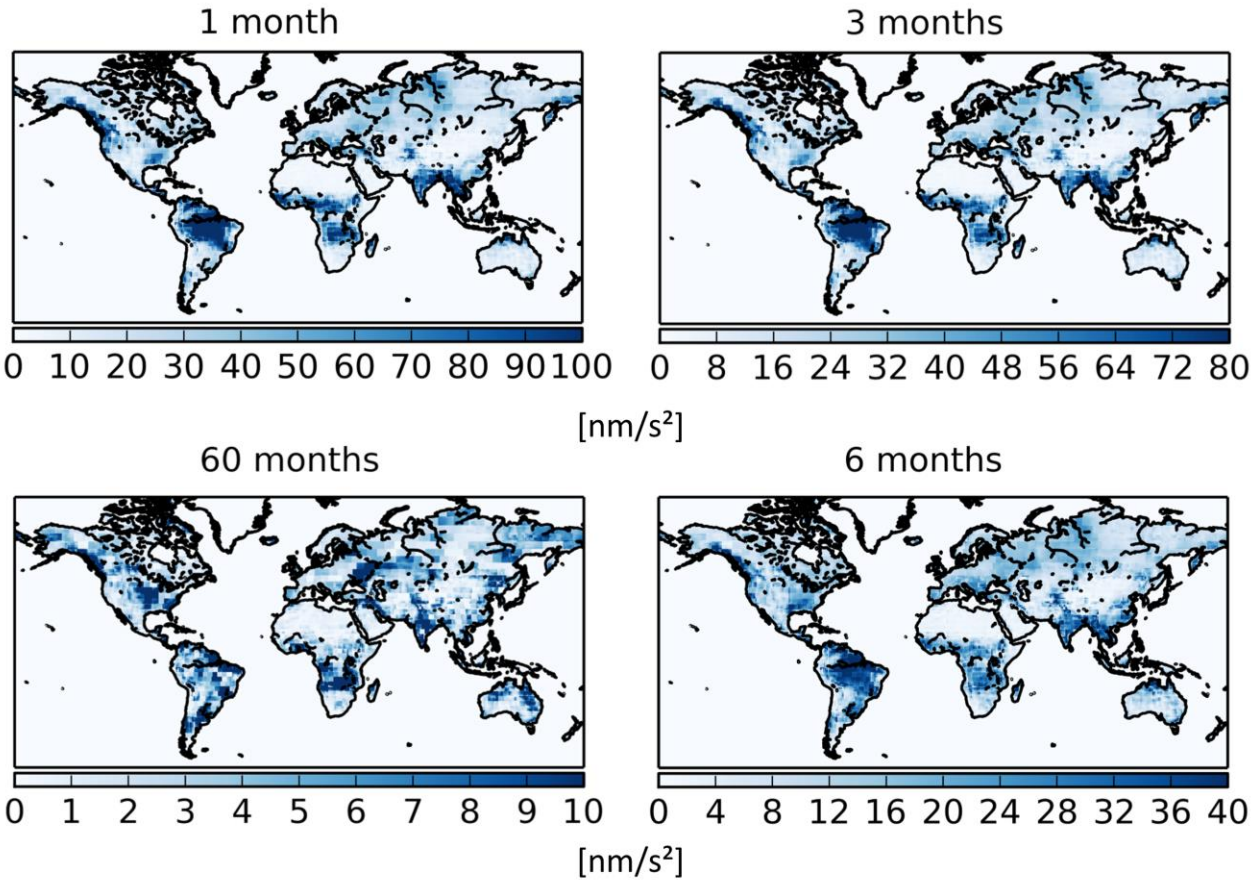

Figure 2. Allan deviations of the hydrological effects on repeated gravity measurements in the whole world, at periods of 1, 3, 6 and 60 months. The hydrological effects are computed using GRACE observations, using the Bouguer conversion ratio of 4.2 nm/s² per cm of water.

4.1 Northwestern Europe

In Northwestern Europe, Belgium and western Germany lie in a zone where GRACE indicates a 12-month Allan standard deviation of 7 nm/s². Adding up the AG setup noise, one obtains 17.5 nm/s². This uncertainty compares with the one deduced from our repeated AG measurements that provide standard deviations ranging 16-24 nm/s².

To better estimate this effect, as well as the influence of the number of repeated AG measurements on the trend estimate, we simulated yearly measurements performed 2, 3, 5 and 10

times, for durations of 2, 3, 5 and 10 years by randomly picking data from the GRACE mascon solution.

To estimate the variability of the trend, we randomly pick 5,000,000 places in the area of interest and starting dates (distributed from 30 days before to 30 days after October, 1); then we compute the trend obtained from the GRACE models for those places. October 1st is chosen because most of the yearly AG measurements relevant for this study are acquired around that time of the year. Concurrently to the interannual mass variability effects, the instrumental setup noise is taken into account by adding a normal random variable with a standard deviation of 16 nm/s². Table S1 provides a standard deviation averaged on the zones shown on Figures 1 and S1.

We also made similar simulations at the AG stations, for which we picked randomly 100,000 sets of N dates, around October 1st, distributed over D years (N, D= 2, 3, 5 and 10, $D \geq N$). For the resulting time series, we estimate the standard deviation of the GRACE time series closest to the station. We end up with an average standard deviation of 1.5±0.3 nm/s²/a after 10 years of yearly measurements, which compares well with the actual average standard deviation of 1.6±1.4 nm/s²/a reported at the 9 AG stations (see Table 2 in *Van Camp* et al. [2011]). Considering that GRACE does not represent precisely the space-time mass distribution near the stations, and that the experimental setup is not exactly that reproduced in our test, we consider that the results of this simulation are close enough to observation to be convincing and to validate our approach.

Table S1 shows that, everywhere in the world, at least 5 AG measurements are needed over a 10 year period to achieve an uncertainty smaller than 10 nm/s²/a at the one sigma level. This becomes less than 5 nm/s²/a, provided one measurement is performed each year.

4.2 Canada, northern USA

In North America, the AG stations from the study of *Lambert* et al. [2013a; 2013b] and *Mazzotti* et al. [2011] lie in a zone where GRACE indicates a 12-month Allan deviation ranging 5 nm/s² (Priddis, Alberta) to 37 nm/s² (Wausau, Wisconsin). Taking into account the AG setup noise of 16 nm/s², one obtains 28-40 nm/s², which compares with the uncertainties of yearly repeated AG measurements that provide standard deviations ranging 25-37 nm/s² (digitized data from the Figures 3a-3e in *Lambert* et al. [2005]). After 10 years, the uncertainties on the slopes range 1-3 nm/s²/a, which agrees with *Mazzotti* et al. [2011] reporting on uncertainties ranging 1-4 nm/s²/a.

4.3 Southern Tibet

In southern Tibet, *Chen* et al. [2016] reported on gravity differences of -21, 62, 70 and 407 nm/s², at 4 stations, based on measurements performed first in October 2010 or August 2011, and repeated once in July 2013. However, this zone experiences strong loading effects from seasonal water storage changes and hydrological changes over the longer term [*Chanard* et al., 2015; *Hao et al.*, 2016; *Rodell et al.*, 2009]. The 12-months Allan standard deviations, which indicate the interannual variability, are 26, 17, 17, 21 nm/s² at Naqu, Lhasa, Shigatse and Zhongba, respectively. There are large differences in monsoon rainfall between July-August (about 120 mm of water per month in Lhasa) and October (10 mm of water per month), which can induce additional hydrological effects at the 20 nm/s² level, according to the 1-month Allan deviation. To account for this variability, another simulation of the uncertainty affecting the slope estimate was performed. This includes the setup noise, considering 60 days before and after October 1 (Table S2). We end up with standard deviations of 32, 24, 20 and 28 nm/s²/a at Naqu, Lhasa, Shigatse and Zhongba, respectively. This is enough to account for the claimed gravity changes at all stations but Shigatse.

Note that the monsoon effects can dramatically be amplified by local hydrogeological effects such as floods in valleys, response of local aquifers, lakes, endorheic lakes and alluvial plains; or mudflows, landslides and deposits, which may play an important role, especially in the Tibetan rugged terrain. This cannot be observed directly by GRACE, and requires local investigation, as done for example by *Mouyen* et al. [2013]. That paper reports on repeated AG measurements in Taiwan where the observed gravity changes range -410 to +2850 nm/s², induced by landslides and sediment accumulation triggered by a typhoon. Given the large AG changes at Shigatse station do not coincide with any signal in the GRACE data, we believe, like *Yi et al.* [2016] that it must reflect a local effect related either of hydrology or mass redistribution by surface processes.

Sun et al. [2009] also reported repeated measurements in Tibet at three stations, performed between 1990 and 2008 at the same epoch of the year: Lhasa (4 and 3 measurements on two different points, -19.7 nm/s²/a), Kunming (6 measurements, -14.2 nm/s²/a) and Dali (10 measurements, -4.1 nm/s²/a). Combining the hydrological effects and the setup noise, we obtain uncertainties on the trend of 3, 9 and 2 nm/s²/a, considering that measurements were made within ±30 days around October 1. Lhasa and, possibly, Dali may have experienced a gravity rate too large (above the two-sigma level) to relate to climate dynamics. However, in these two studies in Tibet, different instruments were used. *Chen* et al. [2016] made use of at least two different absolute gravimeters (one FG5 and one A10), while *Sun* et al. [2009] used 5 different ones in Lhasa, 2 in Kunming and 4 in Dali. This induces instrumental artefacts at a level that can reach the observed signal: the reported differences affecting FG5 and JILAg instruments range up to 134 nm/s², and up to 461 nm/s² for A10 gravimeters. In particular, *Francis et al.* [1995] report on results from JILAg 3 and 5 instruments used by *Sun et al.* [2009]: difference of about 100 nm/s²

is observed between the two instruments, and unrealistic trends in Brussels (300 nm/s² in 6 years) and Membach (eastern Belgium, 100 nm/s² in 3 years) could never be confirmed later on [*Van Camp et al.*, 2011]. Hence, the tectonic interpretations of *Sun* et al. [2009] and *Chen* et al. [2016] are questionable in our opinion, especially when the still experimental JILAg and early FG5 instruments are taken into account. A detailed discussion on the offsets and uncertainties of JILAg and early FG5 gravimeters are given by *Palinkas et al.* [2012]. Moreover, in Lhasa, the trend is the average of two trends recorded at two different places, 800 m apart. Differences in the gravity response to local hydrogeological effects at sites only 40 meters apart have been reported to be as large as 100 nm/s² within a few months [*Mikolaj et al.*, 2015]. Hence, averaging two trends, including one determined on only three measurements, is questionable.

4.4 Other zones

As shown by the Tables S1 and S2, in most of the cases, one needs at least 5 repeated AG measurements during 10 years to achieve an uncertainty on the determination of a trend lower than 10 nm/s²/a, at the one-sigma level. This decreases down to 3-4 nm/s² if the 10 yearly measurements are performed. On the other hand, it is hopeless to achieve a precision better than 20 nm/s²/a, if only 3 measurements are performed during 3 years. Given that measurements are usually not performed at exactly the same date of the year, degrees of freedom of +/-30 and +/-60 days were taken into account. The 60 days cases are slightly noisier, but the increase remains under the 10% level. However, those GRACE-inferred estimates represent average values in the geographic zones shown on Figures 1 and S1. They do not represent local phenomena, where hydrogeological effects may affect gravity at the 100-150 nm/s² level, sometimes within a few hours [*Van Camp et al.*, 2006b; *Meurers et al.*, 2007]. Our results can thus be considered as a lower bound of the climate-induced mass transfer uncertainty.

5 Conclusions

The ground water content inferred from GRACE mascon JPL solutions was used to estimate the time variations of hydrological signals in repeated absolute gravity measurements. This was done everywhere in the world, and the results are discussed in three zones where papers report on repeated AG measurements: Northwestern Europe, Canada and Tibet. Taking into account the instrumental setup noise, different time intervals (2, 3, 5, 10 years) and different numbers of AG campaigns (2, 3, 5, 10), we estimate uncertainties affecting the determination of a linear gravity rate of change. For 10 yearly campaigns, performed during the same epoch of the year, an average uncertainty ranging 3-4 $nm/s^2/a$ can be achieved in most of the cases, in the absence of instrumental artefacts and of strong local hydrogeological effects.

The results are consistent with the amplitude of observed gravity changes on long term repeated campaigns, provided the measurement were performed with the same instrument. This allows extrapolating our simulation at different locations in the world. They invite care regarding the interpretation of results from short campaigns, and even more so in area prone to fluctuations of hydrology and mass redistribution by surface processes. Poor calibration of the gravimeters may dramatically affect this result. We draw attention on the possible offsets which can significantly influence the repeated AG measurements when different instruments are used. Finally, in this study, a linear trend was removed from the GRACE time series. Separating trends induced by long term climate change effects from tectonic signals is a difficult issue not addressed in this study.

Acknowledgments and Data

The data used in the references, tables and supplements and repository at http://podaac.jpl.nasa.gov/dataset/TELLUS_GRACE_MASCON_CRI_GRID_RL05_V1. We thank Reinhard Falk (BKG) and Michal Mikolaj (GFZ Potsdam), two anonymous reviewers and the editor Andrew Newman for fruitful discussions. The work of OdV was supported by the Institut Universitaire de France, and by the CNES as an exploitation of the GRACE space gravity mission.

References

Allan, D. W. (1966), The statistics of atomic frequency standards, *Proc. IEEE*, 54(2), 221–230.

Bettinelli, P., J. P. Avouac, M. Flouzat, L. Bollinger, G. Ramillien, S. Rajaure, and S. Sapkota (2008), Seasonal variations of seismicity and geodetic strain in the Himalaya induced by surface hydrology, *Earth Planet. Sci. Lett.*, *266*(3-4), 332-344.

Blewitt, G., D. Lavalee, P. Clarke, and K. Nurutdinov (2001), A new global mode of Earth deformation: Seasonal cycle detected, Science, *294*(5550), 2342-2345.

Chanard, K., J. P. Avouac, G. Ramillien, and J. Genrich (2014), Modeling deformation induced by seasonal variations of continental water in the Himalaya region: Sensitivity to Earth elastic structure, *J. Geophys. Res. Solid Earth*, *119*, doi:10.1002/2013JB010451.

Chen, S., M. Liu, L. Xing, W. Xu, W. Wang, Y. Zhu, and H. Li (2016), Gravity increase before the 2015 Mw 7.8 Nepal earthquake, *Geophys. Res. Lett.*, *43*, doi:10.1002/2015GL066595.

318 Creutzfeldt, B., A. Güntner, T. Klügel, and H. Wziontek (2008), Simulating the influence of
319 water storage changes on the superconducting gravimeter of the Geodetic Observatory
320 Wettzell, Germany, *Geophysics*, *73*(6), doi: 10.1190/1.2992508.

321 Creutzfeldt, B., A. Güntner, H. Thoss, B. Merz, and H. Wziontek (2010a), Measuring the effect
322 of local water storage changes on in situ gravity observations: Case study of the Geodetic
323 Observatory Wettzell, Germany, *Water Resour. Res.*, *46*, W08531,
324 doi:10.1029/2009WR008359.

325 Creutzfeldt,B., A. Güntner, H. Wziontek, and B. Merz (2010b), Reducing local hydrology from
326 high-precision gravity measurements: a lysimeter-based approach, *Geophys. J. Int.*, *183*
327 (1): 178-187. doi: 10.1111/j.1365-246X.2010.04742.x.

328 Djamour, Y., P. Vernant, R. Bayer, H. R. Nankali, J.-F. Ritz, J. Hinderer, Y. Hatam, B. Luck, N.
329 Le Moigne, M. Sedighi, and F. Khorrami (2010), GPS and gravity constraints on
330 continental deformation in the Alborz mountain range, Iran, *Geophys. J. Int*., doi:
331 10.1111/j.1365-246X.2010.04811.x.

332 Francis, O., B. Ducarme, F. De Meyer, and J. Mäkinen (1995), Present stage of absolute gravity
333 measurements in Brussels and comparison with the superconducting gravimeter drift, in
334 Proceedings of the Workshop: Non tidal gravity changes: intercomparison between
335 absolute and superconducting gravimeters, September 6– 8, 1994, Walferdange, Grand-
336 Duchy of Luxembourg, *Cah. Cent. Eur. Géodyn. Séismol.*, vol. 11, edited by C. Poitevin,
337 pp. 117–123, Cent. Eur. de Géodyn. et de Sésmol., Luxembourg.

338 Francis, O., et al. (2005), Results of the International Comparison of Absolute Gravimeters in
339 Walferdange (Luxembourg) of November 2003, in *International Association of Geodesy*

Symposia Gravity, Geoid and Space Missions GGSM 2004, Vol. 129 Jekeli, Christopher; Bastos, Luisa; Fernandes, Joana (Eds.), XVI, 368 p, Springer-Verlag, pp272-275.

Francis, O., et al. (2010), Results of the European Comparison of Absolute Gravimeters in Walferdange (Luxembourg) of November 2007, in *Gravity, Geoid and Space Missions, International Association of Geodesy Symposia*, Vol. 135(1), edited by S. P. Mertikas, pp. 31–36, doi:10.1007/978-3-642-10634-7_5, Springer, Berlin.

Francis, O., et al. (2013), The European Comparison of Absolute Gravimeters 2011 (ECAG-2011) in Walferdange, Luxembourg: results and recommendations, *Metrologia*, *50*, (2013) 257–268, doi:10.1088/0026-1394/50/3/257.

Francis, O., et al. (2015), CCM.G-K2 key comparison, *Metrologia*, 52 07009, doi: 10.1088/0026-1394/52/1A/07009.

Hao, M., J. T. Freymueller, Q. Wang, D. Cui, and S. Qin (2016), Vertical crustal movement around the southeastern Tibetan Plateau constrained by GPS and GRACE data, *Earth Planet. Sci. Lett., 437*, 1-8.

Jiang, Z., et al. (2011), Final report on the Seventh International Comparison of Absolute Gravimeters (ICAG 2005), *Metrologia*, *48*,, 246-260, doi: 10.1088/0026-1394/48/5/003.

Jiang, Z., et al. (2012), The 8th International Comparison of Absolute Gravimeters 2009: the first Key Comparison (CCM.G-K1) in the field of absolute gravimetry, *Metrologia*, *49*(6), doi: doi:10.1088/0026-1394/49/6/666.

Jacob, T., R. Bayer, J. Chery, H. Jourde, N. L. Moigne, J.-P. Boy, J. Hinderer, B. Luck, and P. Brunet (2008), Absolute gravity monitoring of water storage variation in a karst aquifer

361 on the larzac plateau (Southern France), *J. Hydrol.*, *359*(1–2), 105–117,
362 doi:10.1016/j.jhydrol.2008.06.020.

363 Lambert, A., N. Courtier, and T.S. James (2006), Long-term monitoring by absolute gravimetry:
364 tides to postglacial rebound, *J. Geodyn.*, *41*(1-3), 307–317,
365 doi:10.1016/j.jog.2005.08.032.

366 Lambert, A., J. Huang, G. van der Kamp, J. Henton, S. Mazzotti, T. S. James, N. Courtier, and
367 A. G. Barr (2013a), Measuring water accumulation rates using GRACE data in areas
368 experiencing glacial isostatic adjustment: The Nelson River basin, *Geophys. Res. Lett.*,
369 *40*, 6118–6122, doi:10.1002/2013GL057973.

370 Lambert, A., J. Henton, S. Mazzotti, J. Huang, T.S. James, N. Courtier, and G. van der Kamp
371 (2013b), Postglacial Rebound and Total Water Storage Variations in the Nelson River
372 Drainage Basin: A Gravity-GPS Study, *Geol. Surv. Can. Open File*, OF 7317, 21 pp.

373 Lampitelli, C., and O. Francis (2010), Hydrological effects on gravity and correlations between
374 gravitational variations and level of the Alzette River at the station of Walferdange,
375 Luxembourg. *J. Geodyn.*, *49*, 31–38.

376 Mazzotti, S., A. Lambert, N. Courtier, L. Nykolaishen, and H. Dragert (2007), Crustal uplift and
377 sea level rise in northern Cascadia from GPS, absolute gravity, and tide gauge data,
378 *Geophys. Res. Lett.*, *34*, L15306, doi:10.1029/2007GL030283.

379 Mazzotti, S., A. Lambert, J. Henton, T. S. James, and N. Courtier (2011), Absolute gravity
380 calibration of GPS velocities and glacial isostatic adjustment in mid-continent North
381 America, *Geophys. Res. Lett.*, *38*, L24311, doi: 10.1029/2011GL049846.

382 Mémin, A., Y. Rogister, J. Hinderer, O.C. Omang, and B. Luck (2011), Secular gravity variation
383 at Svalbard (Norway) from ground observations and GRACE satellite data. *Geophys. J.*
384 *Int.*, 184: 1119–1130. doi: 10.1111/j.1365-246X.2010.04922.x

385 Meurers, B., M. Van Camp, and T. Petermans (2007), Correcting superconducting gravity time-
386 series using rainfall modeling at the Vienna and Membach stations and application to
387 Earth tide analysis, *J. Geod.*, *81*(11), doi:10.1007/s00190-007-0137-1.

388 Mikolaj, M., A. Güntner, M. Reich, S. Schröder, and H. Wziontek (2015), Portable
389 superconducting gravimeter in a field enclosure: first experiences and results, in
390 Proceedings of the Workshop: Hydrology, Geophysics and Geodesy – HG² A new way to
391 manage water resources, October 23, 2015, Brussels, edited by M. Van Camp and M.
392 Vanclooster, pp. 33-55.

393 Mouyen, M., F. Masson, C. Hwang, C.-C. Cheng, N. Le Moigne, C.-W. Lee, R. Kao, and W.-C.
394 Hsieh (2013), Erosion effects assessed by repeated gravity measurements in southern
395 Taiwan, *Geophys. J. Int.*, *192*(1), 113-136. doi: 10.1093/gji/ggs019.

396 Mouyen, M., M. Simoes, F. Mouthereau, F. Masson, C. Hwang, and C.-C. Cheng (2014),
397 Investigating possible gravity change rates expected from long-term deep crustal
398 processes in Taiwan, *Geophys. J. Int.*, *198*(1): 187-197. doi: 10.1093/gji/ggu133.

399 Nicolas, J., J.-M. Nocquet, M. Van Camp, T. Van Dam, J.-P. Boy, J. Hinderer, P. Gegout, E.
400 Calais, M. Amalvict, and E. Calais (2006), Seasonal effect on vertical positioning by
401 satellite laser ranging and global positioning system and on absolute gravity at the OCA
402 geodetic station, Grasse, France, *Geophys. J. Int.*, *167*, 1127–1137.

403 Niebauer, T., G. Sasagawa, J. Faller, R. Hilt, and F. Klopping (1995), A new generation of
404 absolute gravimeters, *Metrologia*, *32*, 159–180, doi:10.1088/0026-1394/32/3/004.

405 Palinkas, V., et al. (2012), Analysis of the repeated absolute gravity measurements in the Czech
406 Republic, Slovakia and Hungary from the period 1991–2010 considering instrumental
407 and hydrological effects, *J. Geod.*, doi: 10.1007/s00190-012-0576-1.

408 Ramillien, G., A. Cazenave, and O. Brunau (2004), Global time variations of hydrological
409 signals from GRACE satellite gravimetry, *Geophys. J. Int.*, *158*(3), 813-826.

410 Rodell, M., et al. (2004), The global land data assimilation system, *Bull. Am. Meteorol. Soc.*, *85*,
411 381–394.

412 Rodell, M., I. Velicogna, and J. S. Famiglietti (2009), Satellite-based estimates of groundwater
413 depletion in India, *Nature*, *460*(7258), 999-1002, doi: 10.1038/nature08238.

414 Sato, T., S. Miura, W. Sun, T. Sugano, J. T. Freymueller, C. F. Larsen, Y. Ohta, H. Fujimoto, D.
415 Inazu, and R. J. Motyka (2012), Gravity and uplift rates observed in southeast Alaska and
416 their comparison with GIA model predictions, *J. Geophys. Res.*, *117*, B01401,
417 doi:10.1029/2011JB008485.

418 Sato, T., J. Okuno, J. Hinderer, D.S. MacMillan, H.P. Plag, O. Francis, R. Falk, and Fukuda Y.
419 (2006), A geophysical interpretation of the secular displacement and gravity rates
420 observed at Ny-Alesund, Svalbard in the Arctic-effects of post-glacial rebound and
421 present-day ice melting, *Geophys. J. Int.*, 165, 729–743, doi: 10.1111/j.1365-
422 246X.2006.02992.x.

423 Santamaría-Gómez, A., and Mémin A. (2015), Geodetic secular velocity errors due to
424 interannual surface loading deformation, *Geophys. J. Int.*, *202*, doi: 10.1093/gji/ggv190.

425 Schmerge, D., et al. (2012), Results of the first North American comparison of absolute
426 gravimeters, NACAG-2010, *J. Geod.*, *86*, doi: 10.1007/s00190-011-0539-y.

427 Steffen, H., O. Gitlein, H. Denker, J. Müller, and L. Timmen (2009), Present rate of uplift in
428 Fennoscandia from GRACE and absolute gravimetry, *Tectonophysics*, *474*(1-2), 69–77,
429 doi:10.1016/j.tecto.2009.01.012.

430 Sun, W., Q. Wang, H. Li, Y. Wang, S. Okubo, D. Shao, D. Liu, and G. Fu (2009), Gravity and
431 GPS measurements reveal mass loss beneath the Tibetan Plateau: Geodetic evidence of
432 increasing crustal thickness, *Geophys. Res. Lett.*, *36*, L02303,
433 doi:10.1029/2008GL036512.

434 Uppala, S.M., et al. (2005), The ERA-40 re-analysis, *Q. J. R. Meteorol. Soc.*, *131*, 2961–3012.

435 Van Camp, M., S. D. P. Williams, and O. Francis (2005), Uncertainty of absolute gravity
436 measurements, *J. Geophys. Res*., *110*, B05406, doi:10.1029/2004JB003497.

437 Van Camp, M., M. Vanclooster, O. Crommen, T. Petermans, K. Verbeeck, B. Meurers, T. van
438 Dam, and A. Dassargues (2006a), Hydrogeological investigations at the Membach
439 station, Belgium, and application to correct long periodic gravity variations, *J. Geophys.*
440 *Res*., *111*, B10403, doi:10.1029/2006JB004405.

441 Van Camp, M., P. Meus, Y. Quinif, O. Kaufmann, M. vanRuymbeke, M. Vandiepenbeck, and T.
442 Camelbeeck (2006b), Karst aquifer investigation using absolute gravity, *Eos Trans. AGU*,
443 *87*(30), 298–298, doi:10.1029/2006EO300005.

444 Van Camp, M., L. Métivier, O. de Viron, B. Meurers, and S. D. P. Williams (2010),
445 Characterizing long-time scale hydrological effects on gravity for improved distinction of
446 tectonic signals, *J. Geophys. Res.*, *115*, B07407, doi:10.1029/2009JB006615.

447 Van Camp, M., O. de Viron, H.-G. Scherneck, K.-G. Hinzen, S. D. P. Williams, T. Lecocq, Y.
448 Quinif, and T. Camelbeeck (2011), Repeated absolute gravity measurements for
449 monitoring slow intraplate vertical deformation in western Europe, *J. Geophys. Res.*, *116*,
450 B08402, doi:10.1029/2010JB008174.

451 Van Camp, M., O. de Viron, and R.J. Warburton (2013), Improving the determination of the
452 gravity rate of change by combining superconducting with absolute gravimeter data,
453 *Comput. Geosci.*, 51, 49-55, doi: 10.1016/j.cageo.2012.07.029.

454 Van Camp M., O. de Viron, L. Métivier, B. Meurers, and O. Francis (2014), The quest for a
455 consistent signal in ground and GRACE gravity time series, *Geophys. J. Int.*, doi:
456 10.1093/gji/ggt524.

457 van Dam, T., J. Wahr, P. C. D. Milly, A. B. Shmakin, G. Blewitt, D. Lavallee, and K. M. Larson
458 (2001), Crustal displacements due to continental water loading, *Geophys. Res. Lett.*,
459 *28*(4), 651-654.

460 Vitushkin, L., et al. (2002), Results of the Sixth International Comparison of Absolute
461 Gravimeters ICAG-2001, *Metrologia*, *39*, 407–424, doi:10.1088/0026-1394/39/5/2.

462 Watkins, M. M., D. N. Wiese, D.-N. Yuan, C. Boening, and F. W. Landerer (2015), Improved
463 methods for observing Earth's time variable mass distribution with GRACE using
464 spherical cap mascons, *J. Geophys. Res. Solid Earth*, *120*, 2648–2671,
465 doi:10.1002/2014JB011547.

466 Wiese D.N, D.-N. Yuan, C. Boening, F. W. Landerer, and M. M. Watkins (2015), JPL GRACE
467 Mascon Ocean, Ice, and Hydrology Equivalent Water Height RL05M.1 CRI Filtered,

Ver. 1. PO.DAAC, CA, USA. Dataset accessed [2016-01-15] at http://dx.doi.org/10.5067/TEMSC-OLCR5.

Wouters, B., Bonin, J. A., Chambers, D. P., Riva, R. E. M., Sasgen, I., and Wahr, J. (2014), GRACE, time-varying gravity, Earth system dynamics and climate change. *Rep. Prog. Phys.*, *77*(11):116801, doi:10.1088/0034-4885/77/11/116801.

Yi, S., Q. Wang, and W. Sun (2016), Is it possible that a gravity increase of 20 μGal yr^{-1} in southern Tibet comes from a wide-range density increase?, Geophys. Res. Lett., 43, doi:10.1002/2015GL067509.

Zerbini, S., B. Richter, F. Rocca, T. van Dam, and F. Matonti (2007), A Combination of Space and Terrestrial Geodetic Techniques to Monitor Land Subsidence: Case Study, the Southeastern Po Plain, Italy, *J. Geophys. Res.*, *112*, B05401, doi:10.1029/2006JB004338.

[Geophysical Research Letters]

Supporting Information for

[

Separating climate-induced mass transfers and instrumental effects from tectonic signal in repeated absolute gravity measurements

]

[M. Van Camp[1], O. de Viron[2], and J.-P. Avouac[3]]

[[1]Royal Observatory of Belgium

[2]U. La Rochelle

[3]Caltech]

Contents of this file

Figures S1 to S2
Tables S1 to S2

Additional Supporting Information (Files uploaded separately)

N/A

Introduction

- This supporting information contains maps of zones which are not directly discussed in the main paper: South America, Central Asia, Africa and Oceania. Figure S2 provides the distributions shown on Figures 1 and S1.The tables S1 and S2 provide detailed uncertainties on the determination of the gravity rate of change as a function of the geographic area, the duration of the measurements and the number of measurements.

506

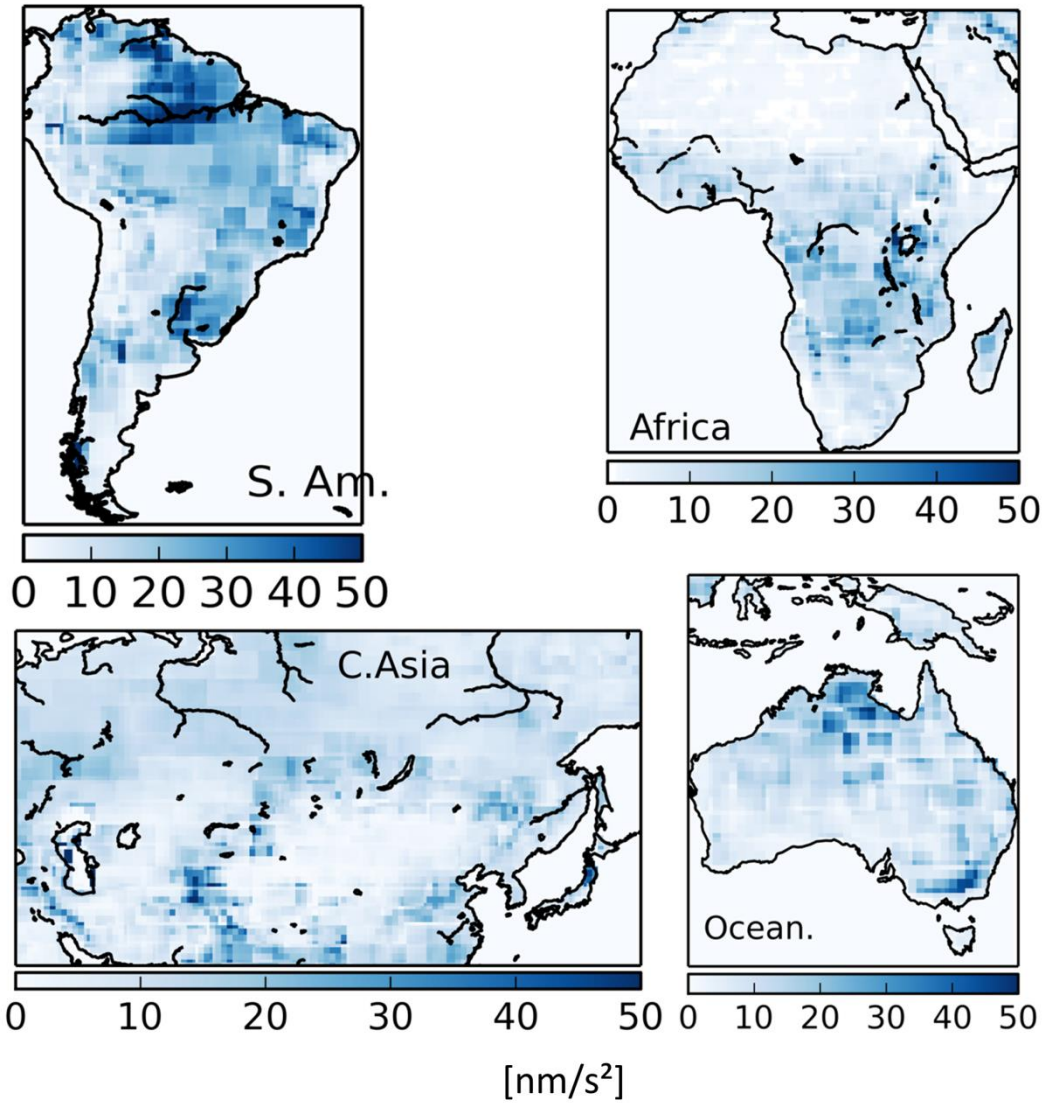

507

508 **Figure S1.** Allan deviations of the hydrological effects on repeated gravity measurements, at the
509 period of 12 months, in South America, Africa, Central Asia and Oceania. The hydrological
510 effects are computed using GRACE observations, using the Bouguer conversion ratio of 4.2
511 nm/s² per cm of water.

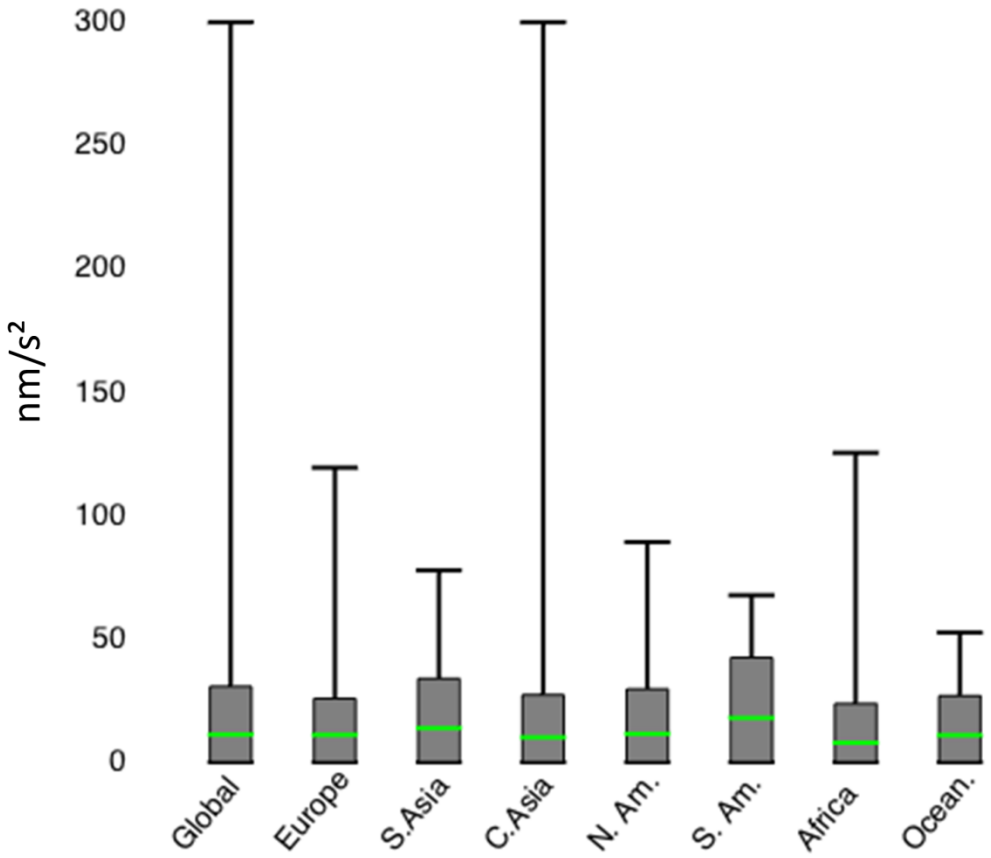

Figure S2. Box and whisker plots of the Allan standard deviations shown on Figures 1 and S1: green line: median (it is indistinguishable from the average); grey boxes: 95% confidence interval; whisker: upper and lower values. Scale in nm/s². Most of the values are under the 50 nm/s² level.

***D* Duration (years)**	***N* Number of measurements**			
World	**2**	**3**	**5**	**10**
10	18	9	5	3
5	24	13	9	-
3	30	18	-	-
2	34	-	-	-
Europe				
10	23	9	5	3
5	24	13	9	-
3	30	19	-	-
2	33	-	-	-
Southeast Asia				
10	27	12	7	4
5	34	19	12	-
3	44	26	-	-
2	50	-	-	-
North America				
10	21	10	5	3
5	28	16	11	-
3	35	22	-	-
2	40	-	-	-
South America				
10	21	10	6	4
5	27	14	10	-
3	34	20	-	-
2	40	-	-	-
Central Asia				
10	20	9	5	3
5	26	14	9	-
3	34	20	-	-
2	39	-	-	-
Africa				
10	19	9	5	3
5	25	14	10	-
3	31	18	-	-
2	35	-	-	-
Oceania				
10	18	9	5	3
5	23	13	9	-
3	30	18	-	-
2	33	-	-	-

Table S1. Standard deviation (in nm/s²/a) of a linear trend due to the hydrological effects as inferred from GRACE, on repeated gravity measurements, performed 2, 3, 5 and 10 times. When relevant, the simulation is done for durations of 2, 3, 5 and 10 years. The standard deviation is obtained by averaging the standard deviations of GRACE observed at all the data

521 points of the selected area, and repeated to sum up to 5 000 000 simulated experiment on the
522 areas shown on Figures 1 and S1. As the gravity measurements cannot be performed exactly at
523 the same day of the year, the simulations allow the measurements to happen randomly from 30
524 before to 30 days after October, 1. In all case an instrumental setup noise of 16 nm/s² is
525 included.
526

D Duration (years)	*N* Number of measurements			
World	**2**	**3**	**5**	**10**
10	18	9	5	3
5	24	14	9	-
3	30	18	-	-
2	34	-	-	-
Europe				
10	18	9	5	3
5	24	14	9	-
3	30	19	-	-
2	34	-	-	-
Southeast Asia				
10	29	14	7	4
5	38	21	14	-
3	49	29	-	-
2	56	-	-	-
North America				
10	22	10	5	3
5	29	17	11	-
3	35	21	-	-
2	41	-	-	-
South America				
10	21	10	6	4
5	28	16	10	-
3	35	21	-	-
2	41	-	-	-
Central Asia				
10	21	10	5	3
5	28	16	10	-
3	36	21	-	-
2	43	-	-	-
Africa				
10	21	10	5	3
5	27	16	11	-
3	34	20	-	-
2	40	-	-	-
Oceania				
10	18	9	5	3
5	23	14	9	-
3	30	18	-	-
2	34	-	-	-

Table S2. Same as Table S1 but allowing the measurements to be performed up to 60 days before and after October 1.